

## 430 A Neurips Checklist Answer Clarification

431 During submission, we were not aware of the guidance for filling the checklist and thus misunderstood  
432 some questions in it. In this section, we want to correct our answers to some of the checklist questions,  
433 if allowed:

- 434 • Broader Impacts: n/a
- 435 • Experiments: yes, and the code can be found at: [https://github.com/elden-neurips2023/](https://github.com/elden-neurips2023/ELDEN)  
436 ELDEN

## 437 B ELDEN details

438 **Assumptions** We summarize our assumptions on the MDP as follows:

- 439 1. The state space can be factored as  $\mathcal{S} = \mathcal{S}^1 \times \dots \times \mathcal{S}^N$ .
- 440 2. The transition of each state factor is independent, i.e., the dynamics can be represented  
441  $\mathcal{P}(s_{t+1}|s_t, a_t) = \prod_{n=1}^N p(s_{t+1}^n | \text{Pa}(\mathcal{S}_{t+1}^n))$ .
- 442 3. There is no instantaneous dependency between state factors at the same time step  $t$ , i.e., no  
443 dependency such as  $s_t^i \rightarrow s_t^j$  for any  $i, j$ .

444 For assumption 1, factored state space is commonly employed in causality literature and is applicable  
445 to many simulated or robotics environments. In cases where low-level observations or partial  
446 observability are present, disentangled representation or causal representation methods can be utilized  
447 to learn a factored state space [16]. When a factored state space is available, assumptions 2 and 3  
448 generally hold.

449 **Network Architecture** In Figure 4(a), the architecture of ELDEN for predicting each state factor  
450  $s_{t+1}^j$  is illustrated. The process consists of the following steps:

- 451 1. Feature Extraction: For each input state factor  $s_t^i$ , ELDEN utilizes a separate multi-layer perception  
452 (MLP) to extract its corresponding feature  $g^i$ .
- 453 2. Entity Interaction: ELDEN employs a multi-head self-attention module to model entity interactions  
454 and generates a set of transformed features  $h^i$  that incorporate information from other state factors.
- 455 3. Prediction using Multi-Head Attention: With  $h^j$  as the query, ELDEN utilizes a multi-head  
456 attention module to compute the prediction  $\hat{p}(s_{t+1}^j | s_t, a_t)$  for each state factor. For continuous  
457 state factor,  $\hat{p}(s_{t+1}^j)$  is modeled as a normal distribution with the mean computed by the network  
458 and a fixed variance equal to 1. For discrete factor,  $\hat{p}(s_{t+1}^j)$  is a categorical distribution with  
459 network outputs as class probabilities.

460 Throughout the prediction process, there are a total of  $N$  such networks in ELDEN, with each network  
461 responsible for predicting a separate state factor  $s_{t+1}^j$ .

462 The training loss for the dynamics model is:

$$L = -\log \prod_{j=1}^N \hat{p}(s_{t+1}^j | s_t, a_t) + \lambda \sum_{i,j} \left| \frac{\partial \hat{p}(s_{t+1}^j)}{\partial s_t^i} \right|, \quad (3)$$

463 where  $\lambda$  is the coefficient for partial derivative regularization.

## 464 C Environment Details

465 In this section, we provide a detailed description of the environment, including its semantic stages  
466 representing internal progress toward task completion, state space, and action space. We also highlight  
467 that while each task consists of multiple semantic stages, agents do not have access to this information.  
468 The learning signal for agents is solely based on a sparse reward of 0 or 1, indicating whether the task  
469 has been completed or not. Additionally, in each environment, the poses of all environment entities  
470 are randomly initialized for each episode.

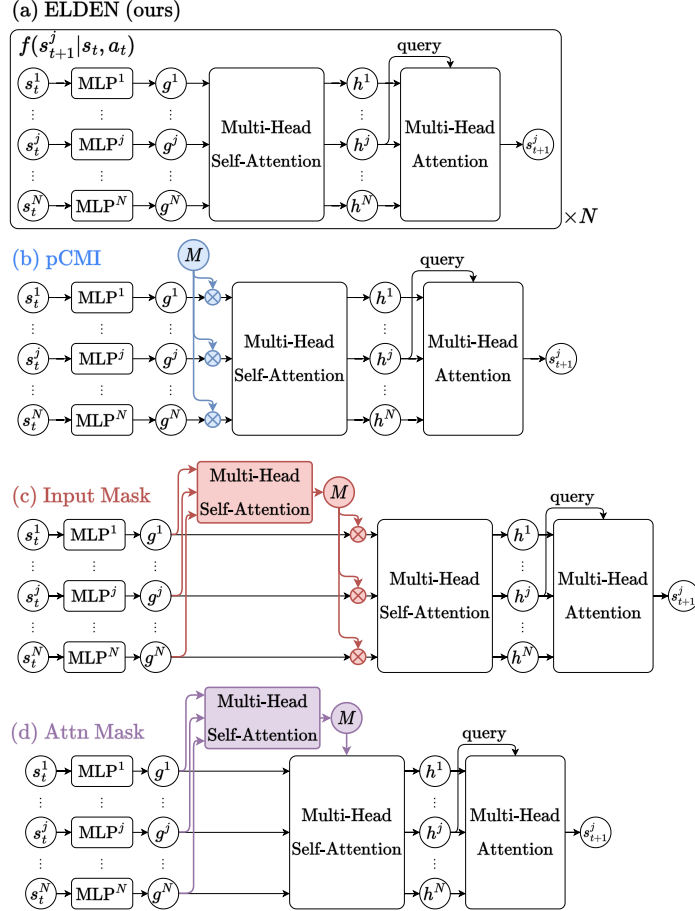


Figure 4: The dynamics model of each local dependency detection method. **(a)** The dynamics model of ELDEN for predicting  $s_{t+1}^j$ . Notice that each network predicts  $s_{t+1}^j$  only, and there are  $N$  such networks in total, each responsible for predicting one state factor in  $s_{t+1}$ . For visual simplicity, the “ $\times N$ ” symbol is only shown in (a). **(b)** pCMI computes  $p(s_{t+1}^j | s_t, a_t)$  and  $p(s_{t+1}^j | s_t \setminus s_t^i, a_t)$  by manually setting the binary mask  $M$  to different values, where  $\otimes$  represents element-wise multiplication. **(c)** For Input Mask,  $M$  is learned to condition on  $(s_t, a_t)$  and is regularized to use as few inputs as possible. **(d)** For Attn Mask,  $M$  also conditions on  $(s_t, a_t)$  but is applied to the attention score in the self-attention module.

471 Meanwhile, as ELDEN focuses on exploring novel local dependencies between environment entities,  
 472 in all environments, the action space consists of hard-coded skills to increase the probability of entity  
 473 interactions and bypass navigation challenges under sparse rewards. Extending ELDEN to explore  
 474 local dependency and learn such skills simultaneously would be an important direction for future  
 475 work.

476 **Thawing** As shown in Fig. 5(a), the Thawing environment consists of a sink, a refrigerator, and a  
 477 frozen fish. The task requires the agent to complete the following **stages**: (1) open the refrigerator, (2)  
 478 take the frozen fish out of the refrigerator, and (3) put the fish into the sink to thaw it. The discrete state  
 479 space consists of (i) the agent’s position and direction, (ii) the positions of all environment entities,  
 480 (iii) the thawing status of the fish, and (iv) whether the refrigerator door is opened. The discrete  
 481 action space consists of (i) moving to a specified environment entity, (ii) picking up / dropping down  
 482 the fish, and (iii) opening / closing the refrigerator door.

483 **CarWash** As shown in Fig. 5(b), the CarWash environment consists of a car, a sink, a bucket, a  
 484 shelf, a rag, and a piece of soap. The task requires the agent to complete the following **stages**: (1)  
 485 take the rag off the shelf, (2) put it in the sink, (3) toggle the sink to soak the rag up, (4) clean the

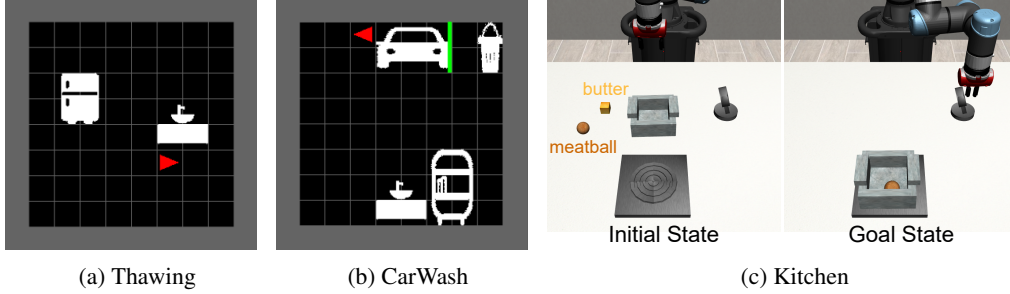


Figure 5: Environments.

486 car with the soaked rag, (5) take the soap off the self, and (6) clean the rag with the soap inside the  
 487 bucket. The discrete state space consists of (i) the agent’s position and direction, (ii) the positions  
 488 of all environment entities, (iii) the soak status of the rag, (iv) the cleanness of the rag and the car,  
 489 and (v) whether the sink is toggled. The discrete action space consists of (i) moving to a specified  
 490 environment entity, (ii) picking up / dropping down the rag, (iii) toggling the sink, and (iii) picking  
 491 up / dropping down the soap.

492 **Kitchen** As shown in Fig. 5(c), in the kitchen environment, there are a robot arm (i.e., the agent), a  
 493 piece of butter, a meatball, a pot, and a stove with its switch. The task requires the agent to complete  
 494 the following **stages**: (1) pick and place the butter into the pot, (2) pick and place the pot onto the  
 495 stove, (3) turn on the stove to melt the butter in the pot, (4) pick and place the meatball into the pot  
 496 to cook it, and (5) turn off the stove. Notice that melting the butter is a prerequisite for cooking the  
 497 meatball, otherwise, it will result in the meatball being overcooked and the task failing. The state  
 498 space is continuous, consisting of the pose of all objects, the melting status of the butter, and the  
 499 cooking status of the meatball (whether it is raw, cooked, or overcooked). The action space is discrete,  
 500 consisting of hard-coded skills: moving to [butter, meatball, pot, pot handle, stove, stove switch],  
 501 grasping, dropping, and toggling the switch. Grasping and toggling are only applicable when the  
 502 end-effector is close to the corresponding environment entities.

## 503 D Evaluating the Detection of Local Dependencies

### 504 D.1 Implementation

505 **Baselines** We give a detailed description of each baseline as follows:

- 506 • **pCMI** (point-wise conditional mutual information): it considers that the local dependency  
 507  $s_t^i \rightarrow s_{t+1}^j$  exists if their point-wise conditional mutual information is greater than a predefined  
 508 threshold, i.e.,  $\text{pCMI}^{i,j} := \log \frac{p(s_{t+1}^j | s_t, a_t)}{p(s_{t+1}^j | s_t \setminus s_t^i, a_t)} \geq \epsilon$ . As shown in Fig. 4(b), to compute  $\text{pCMI}^{i,j}$ ,  
 509 Wang et al. [32] uses a manually defined binary mask  $M \in [0, 1]^N$  to ignore some inputs when  
 510 predicting  $s_{t+1}^j$ : (1) to compute  $p(s_{t+1}^j | s_t, a_t)$ ,  $M$  uses all inputs (all its entries are set to 1),  
 511 and (2) to compute  $p(s_{t+1}^j | s_t \setminus s_t^i, a_t)$ , the entry for  $g^i$  is set to 0. When evaluating the local  
 512 dependency, pCMI needs to compute  $p(s_{t+1}^j | s_t \setminus s_t^i, a_t)$  for every  $i$ , and thus its computation  
 513 cost is  $N$  times larger than ELDEN. We also compute pCMI following Seitzer et al. [27], which  
 514 yields similar performance but is even more computationally expensive compared to the method  
 515 proposed by Wang et al. [32].
- 516 • **Attn** (attention): it uses the same architecture as ELDEN that is shown in Fig. 4(a). When  
 517 computing the overall attention score, it averages the attention score across all heads in each  
 518 module, then computes the likelihood of dependency  $s_t^i \rightarrow s_{t+1}^j$  as  $\sum_{k=1}^N c^{g^i, h^k} \cdot c^{h^k, s_{t+1}^j}$  where  
 519  $c^{a,b}$  is the averaged score between the input  $a$  and the output  $b$ .
- 520 • **Input Mask**: as shown in Fig. 4(c), it also uses a binary mask  $M$  except that  $M$  is computed  
 521 from  $(s_t, a_t)$ . During training, to only use necessary inputs for  $s_{t+1}^j$  prediction,  $M$  is regularized  
 522 with the L1 norm on its number of non-zero entries. The Gumbel reparameterization is used to  
 523 compute the gradient for the binary  $M$  [11].

Table 2: Parameters of the dynamics model training for local dependency detection experiments. Parameters shared if not specified.

Name		Tasks		
		Thawing	CarWash	Kitchen
environment	episode length	20	100	100
	grid size	10	10	N/A
training	optimizer		Adam	
	learning rate		$3 \times 10^{-4}$	
	batch size		32	
	# of training batches		500k	
	# of random seeds		3	
	mixup Beta parameter	1	1	N/A
ELDEN	activation functions		ReLU	
	$\{\text{MLP}\}_{i=1}^N$	[64, 64]	[64, 64]	[128, 128]
	$\lambda$ annealing starts	50k	50k	100k
	$\lambda$ annealing ends	100k	100k	200k
	# of heads		4	
	use bias		False	
	attention key, query, value size	16	16	32
	output size	64	64	128
	post attn MLP	[64, 64]	[64, 64]	[128, 128]
Input Mask	attention parameters		same as ELDEN	
	$M$ regularization coefficient		$1 \times 10^{-2}$	
	$M$ regularization annealing starts	50k	50k	100k
	$M$ regularization annealing ends	100k	100k	200k
Attn Mask	attention parameters		same as ELDEN	
	signature size		64	
	SKPMD learnable bandwidth		True	
	bandwidth initialization		1	

524 • **Attn Mask:** as shown in Fig. 4(d), similar to Input Mask, a mask  $M$  of size  $N \times N$  is computed  
525 from  $(s_t, a_t)$ , but it is applied to the attention score. The mask is regularized with Stochastic  
526 Kernel Modulated Dot-Product (SKMDP) proposed by Weiss et al. [33].

527 For modules that are shared by all methods, we use the same architecture for a fair comparison.

528 **Data** For a fair comparison, when training each method, we use the same dataset collected by  
529 a scripted policy, rather than let each method collect its own data, to avoid potential performance  
530 differences caused by data discrepancies. Specifically, we use a scripted policy to expose all potential  
531 local dependencies and collect 500K transitions in each environment.

532 Notice that, in exploration with sparse reward experiments, the dynamics models are still trained  
533 online, using the transition data collected on its own.

534 **Hyperparameters** The hyperparameters used for evaluating local dependency detection of each  
535 method are provided in Table 2. Unless specified otherwise, the parameters are shared across all  
536 environments.

## 537 D.2 Ablation of Mixup and Partial Derivative Regularization

538 In our ablation study on ELDEN for local dependency detection, we investigate the impact of each  
539 component with the following variations:

- 540 • **No Mixup & No Reg:** We disable the use of Mixup for discrete space prediction, and no partial  
541 derivative regularization is applied in this case.
- 542 • **Different partial derivative regularization coefficients:** we test with different  $\lambda$  values in  
543  $\{0, 10^{-1}, 10^{-2}, 10^{-3}, 10^{-4}, 10^{-5}\}$ .

Table 3: Ablation of ELDEN on local dependency detection

	THAWING		CARWASH		KITCHEN	
	ROC AUC	F1	ROC AUC	F1	ROC AUC	F1
no Mixup & no Reg	0.48 ± 0.01	0.42 ± 0.01	0.44 ± 0.00	0.27 ± 0.01	N/A	N/A
no Reg, i.e., $\lambda = 0$	0.57 ± 0.01	0.52 ± 0.01	0.54 ± 0.01	0.42 ± 0.01	0.64 ± 0.01	0.24 ± 0.01
$\lambda = 10^{-1}$	0.68 ± 0.00	<b>0.57</b> ± 0.00	0.73 ± 0.01	0.58 ± 0.02	0.55 ± 0.00	0.14 ± 0.00
$\lambda = 10^{-2}$	<b>0.71</b> ± 0.01	<b>0.57</b> ± 0.00	0.76 ± 0.01	0.60 ± 0.00	0.60 ± 0.01	0.21 ± 0.01
$\lambda = 10^{-3}$	0.64 ± 0.01	0.55 ± 0.01	<b>0.78</b> ± 0.02	<b>0.66</b> ± 0.02	0.65 ± 0.00	0.24 ± 0.01
$\lambda = 10^{-4}$	0.65 ± 0.02	0.55 ± 0.01	0.75 ± 0.01	0.60 ± 0.01	<b>0.66</b> ± 0.00	<b>0.25</b> ± 0.01
$\lambda = 10^{-5}$	0.63 ± 0.00	0.53 ± 0.01	0.72 ± 0.00	0.57 ± 0.00	0.65 ± 0.01	0.24 ± 0.01

Table 4: Parameters of the Policy Learning. Parameters shared if not specified.

	Name	Tasks		
		Thawing	CarWash	Kitchen
PPO	optimizer		Adam	
	activation functions		Tanh	
	learning rate		$1 \times 10^{-4}$	
	batch size		32	
	clip ratio		0.1	
	MLP size		[128, 128]	
	GAE $\lambda$		0.98	
	target steps		250	
	n steps	60	600	100
	# of environments	20	20	80
training	# of random seeds		3	
	intrinsic reward coefficient		1	
	# of dynamics update per policy step		1	
	dynamics learning rate		$1 \times 10^{-5}$	
	ensemble size		5	
	PER level of prioritization	N/A	N/A	0.5
	mixup Beta parameter	0.1	0.1	N/A
	partial derivative threshold $\epsilon$		$3 \times 10^{-4}$	

544 As shown in Table. 3, in Thawing and CarWash environments, partial derivative regularization with  
545 appropriate coefficients significantly improves ELDEN’s detection on local dependencies, compared  
546 to no regularization (i.e.,  $\lambda = 0$ ) or inappropriate  $\lambda$  values. Furthermore, in these discrete-state  
547 environments, the use of Mixup is crucial — even when compared to using Mixup without any  
548 regularization, not using Mixup leads to a noticeable degradation in the prediction performance.

## 549 E Evaluating Exploration in Sparse-Reward RL Tasks

### 550 E.1 Implementation

551 During policy learning, all methods share the same PPO and training hyperparameters, provided in  
552 Table 4. The hyperparameters for dynamics model setup during policy learning are the same as in  
553 Table 2 unless specified otherwise.

### 554 E.2 Ablation of Local Dependency Metrics

555 In this section, we compare the exploration performance when using different local dependency  
556 detection methods. Specifically, we compare with pCMI as it achieves best local dependency detection  
557 in Sec. 4.1. We present the comparison results between ELDEN and pCMI in the Kitchen environment  
558 in Fig. 6(a) where both methods successfully learn to solve the task. However, it is important to

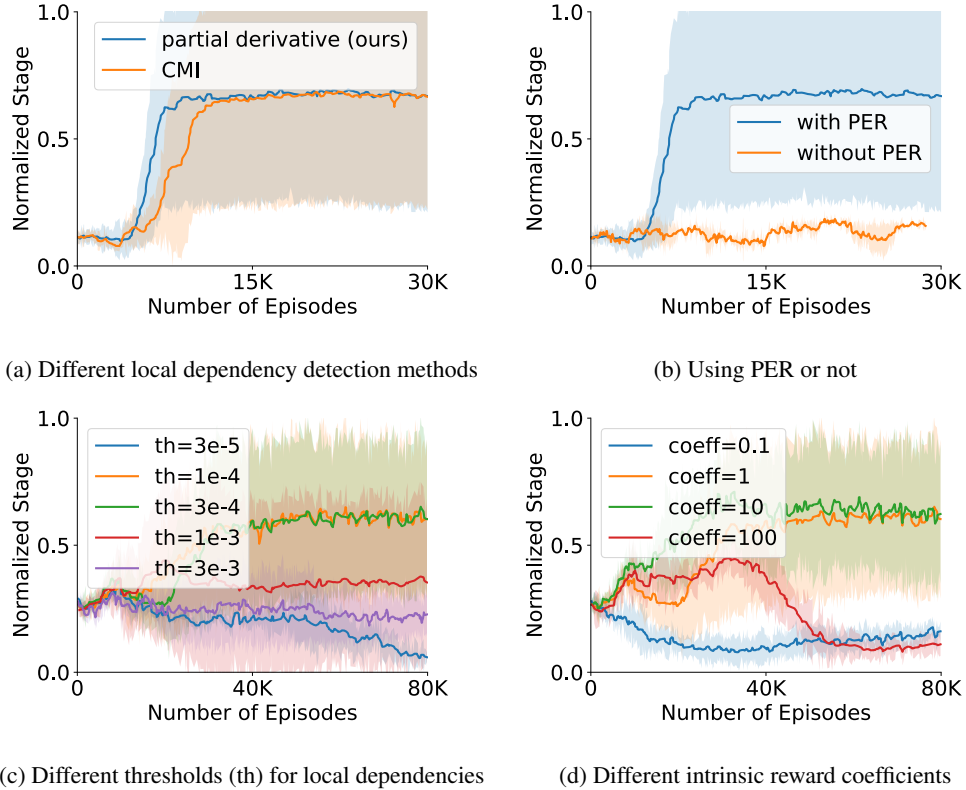


Figure 6: Ablation of ELDEN on task learning.

559 notice that the computation cost of pCMI is  $N$  times more than ELDEN, and thus may not scale to  
 560 environments with a large number of entities.

### 561 E.3 Ablation of Prioritized Experience Replay

562 We study the effectiveness of Prioritized Experience Replay (PER) on task learning. Specifically,  
 563 we test ELDEN with and without PER in the Kitchen environment, and show the result in Fig. 6(b).  
 564 We can see that ELDEN without PER fails to learn useful policy. The reason is some key entity  
 565 interactions occur rather rarely before the agent masters them, e.g., there is a small chance for  
 566 the agent to cook the meatball with random actions. Hence, PER helps the dynamics model learn  
 567 such infrequent dependencies quickly, enabling it to bias the exploration toward reproducing such  
 568 dependencies.

### 569 E.4 Ablation of Partial Derivative Threshold

570 The partial derivative threshold  $\epsilon$  determines the dependencies predictions. A threshold that is too  
 571 large / too small will make all dependency predictions negative / positive respectively, leading to  
 572 deteriorated performance. In this section, we examine whether our method is sensitive to the choice  
 573 of threshold in the CarWash environment, where the results are presented in Fig. 6(c). We observe  
 574 that our method is relatively sensitive to the choice of threshold, and an inappropriate threshold could  
 575 cause catastrophic failure. A potential next step for ELDEN is to automatically determine the partial  
 576 derivative threshold.

### 577 E.5 Ablation of Intrinsic Reward Coefficient

578 The intrinsic reward coefficient controls the scale of the intrinsic reward relative to the task reward.  
 579 We examine the effect of this coefficient by experimenting with different values in the CarWash  
 580 environment, where the results are presented in Fig. 6(d). We find that our methods work well in a

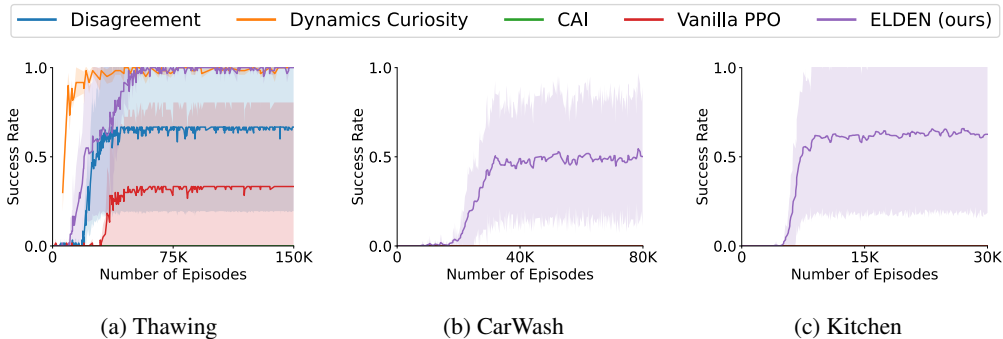
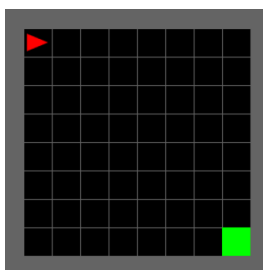
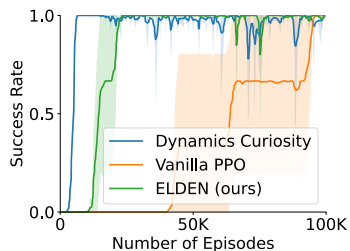


Figure 7: Learning curve of ELDEN (ours) compared to baseline approaches (mean  $\pm$  std dev of success rate across three random seeds). For both CarWash and Kitchen, the success rates for all baselines are zero throughout the training, overlapping with the x axis.



(a) a navigation task with the goal in green



(b) ELDEN performs worse than Dynamics Curiosity

Figure 8: We demonstrate a failure mode of our method on a navigation task.

581 large range of the intrinsic reward coefficients (1 - 10), since the task only gives sparse rewards and  
 582 the intrinsic rewards are the only learning signal most of the time. The only exceptions are (1) when  
 583 the intrinsic reward coefficient is too large (e.g., 100), the intrinsic reward significantly surpasses the  
 584 task reward, and (2) when the coefficient is too small (e.g., 0.1), the episode intrinsic reward will also  
 585 be too small (e.g., 0.03) for PPO to learn any useful policy.

## 586 E.6 Success Rate Plots

587 As a supplementary to the normalized stage metric used in the main paper, we provide the success  
 588 rate as an additional metric. The success rate learning curves of all methods in the three environments  
 589 are shown in in Fig. 7. Again, ELDEN outperforms and performs comparably with all baselines.  
 590 Notice that, in the CarWash and Kitchen environments, all baselines never succeed throughout the  
 591 training (i.e., success rate = 0 for all episodes), leading to training curves that overlap with the x axis.

## 592 F Failure Modes of ELDEN

593 As mentioned in the main paper, ELDEN may have limited advantages for tasks that require precise  
 594 control of a specific environment entity. One such example is navigation, where the agent needs to  
 595 reach a very specific point in space that has no particular semantic meaning. We empirically examine  
 596 this statement in the Minigrid environment [7], where the agent needs to navigate to the green goal  
 597 point in an empty room through primitive actions (turn left, turn right, and move forward), as shown  
 598 in Fig. 8(a). We compare ELDEN against Dynamics Curiosity and Vanilla PPO, and present the result  
 599 in Fig. 8(b). Since this environment is relatively simple, all three methods are eventually able to solve  
 600 the task. However, the Dynamics Curiosity converges faster than ELDEN, showing that ELDEN is  
 601 indeed not as capable as curiosity-driven explorations in tasks that focus on precise control rather than  
 602 exploring dependencies between environment entities. The Vanilla PPO converges slowest, indicating  
 603 that even in the Empty environment, ELDEN still has advantages over purely random exploration.

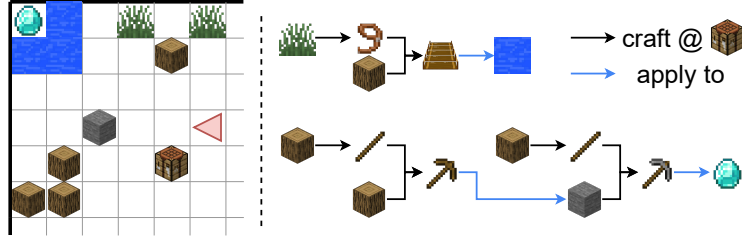


Figure 9: **(Left)** A visualization of the 2-d Minecraft environment. **(Right)** To get the gem, the agent needs to (top) craft a bridge to get across the river, and (bottom) craft a stone pickaxe that is required to collect the gem.

## 604 G Minecraft 2D

605 We also evaluate all exploration methods in a discrete 2-d Minecraft environment that exhibits more  
 606 objects and more complex entity dependencies than Thawing and CarWash. The environment is  
 607 modified from the one used by Andreas et al. [1]. Due to limited space in the paper, we chose to show  
 608 the results in the appendix.

### 609 G.1 Environment Details

610 As shown in Fig. 9, the environment has complex chained  
 611 dependencies — to get the gem, the agent needs to

- 612 1. get across the river to reach the gem by
  - 613 (a) collecting a unit of grass and crafting a rope,
  - 614 (b) collecting a unit of wood and crafting a bridge  
 615 with the rope,
  - 616 (c) building the bridge on top of the river;
- 617 2. collect the gem by
  - 618 (a) collecting a unit of wood to craft a wood stick
  - 619 (b) collecting another unit of wood and combining  
 620 it with the stick to craft a wood pickaxe that is  
 621 required for collecting the stone,
  - 622 (c) collecting a unit of wood and a unit of stone to  
 623 craft a stick and then a stone pickaxe that is re-  
 624 quired for collecting the gem,
  - 625 (d) collecting the gem with the stone pickaxe.

626 Notice that all crafting must be conducted at the crafting  
 627 table. The discrete state space consists of (i) the agent’s  
 628 position and direction, (ii) an inventory tracking the number of materials and tools that the agent  
 629 has, and (iii) the positions of all environment entities. The discrete action consists of (i) picking up /  
 630 applying tools to (only effective when the agent faces an environment entity and has the necessary  
 631 tools to interact with it), (ii) crafting a specified tool (only effective when the agent has enough  
 632 materials and faces the crafting table), and (iii) moving to a specified environment entity.

### 633 G.2 Evaluating Exploration in 2-d Minecraft with Sparse Rewards

634 As shown in Fig. 10, even though the task requires that the agent follows the complex craft procedure  
 635 with complex chained dependencies, ELDEN still learns to finish the task. In contrast, other  
 636 exploration method fails to finish the task, only ending up with crafting one or two useful tools. This  
 637 result again demonstrates ELDEN’s advantage in exploring complex interactions between a large  
 638 number of environment entities.

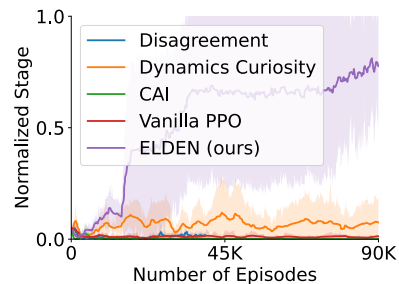


Figure 10: Learning curve of ELDEN (ours) compared to baseline approaches (mean  $\pm$  std dev of the number of stages completed across three random seeds) in the 2-d Minecraft environment.

639 **H Compute Architecture**

640 The experiments were conducted on machines of the following configurations:

- 641 • Nvidia 2080 Ti GPU; AMD Ryzen Threadripper 3970X 32-Core Processor
- 642 • Nvidia A40 GPU; Intel(R) Xeon(R) Gold 6342 CPU @2.80GHz
- 643 • Nvidia A100 GPU; Intel(R) Xeon(R) Gold 6342 CPU @2.80GHz